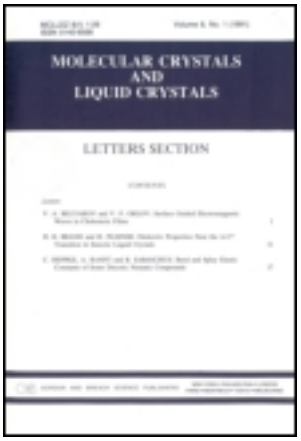

Molecular Crystals and Liquid Crystals
Publication details, including instructions for authors and subscription information:
http://www.tandfonline.com/loi/gmcl20

Effect of Flexible Chain Length on the Photoorientation Behavior of Surface-Grafted Liquid Crystalline Azobenzene Block Copolymer Brush

Hafiz Ashraful Haque [a], Shusaku Nagano [b c] & Takahiro Seki [a]
[a] Department of Molecular Design and Engineering, Graduate School of Engineering, Nagoya University, Furo-cho, Chikusa, Nagoya, 464-8603, Japan
[b] Venture Business Laboratory, Nagoya University, Japan
[c] Japan Science and Technology Agency-PRESTO, Japan
Published online: 16 Dec 2013.

To cite this article: Hafiz Ashraful Haque, Shusaku Nagano & Takahiro Seki (2013) Effect of Flexible Chain Length on the Photoorientation Behavior of Surface-Grafted Liquid Crystalline Azobenzene Block Copolymer Brush, Molecular Crystals and Liquid Crystals, 583:1, 10-20, DOI: 10.1080/15421406.2013.843766

To link to this article: http://dx.doi.org/10.1080/15421406.2013.843766

Mol. Cryst. Liq. Cryst., Vol. 583: pp. 10–20, 2013

ISSN: 1542-1406 print/1563-5287 online
DOI: 10.1080/15421406.2013.843766

Effect of Flexible Chain Length on the Photoorientation Behavior of Surface-Grafted Liquid Crystalline Azobenzene Block Copolymer Brush

HAFIZ ASHRAFUL HAQUE,[1] SHUSAKU NAGANO,[2,3] AND TAKAHIRO SEKI[1,*]

[1]Department of Molecular Design and Engineering, Graduate School of Engineering, Nagoya University, Furo-cho, Chikusa, Nagoya 464-8603, Japan
[2]Venture Business Laboratory, Nagoya University, Japan
[3]Japan Science and Technology Agency-PRESTO, Japan

A liquid crystalline (LC) azobenzene homopolymer brush film of poly[4-(10-methacryloxydecyloxy)-4′-pentylazobenzene] (P5Az10MA), and two diblock copolymer brushes consisting of the same LC azobenzene (Az) block connected with poly(hexyl methacrylate) block (PHMA-b-P5Az10MA) have been synthesized on initiator-immobilized quartz surfaces by atom transfer radical polymerization. In the diblock polymer brushes, the length of PHMA blocks tethering to the substrate surface were changed (26 nm and 51 nm). The orientation and structural features of the liquid crystalline block, containing an Az mesogenic group of the polymer brushes were evaluated by UV-vis spectroscopy and grazing incident X-ray diffraction measurements. Upon irradiation with 436 nm linearly polarized light (LPL), the levels of photoinduced in-plane anisotropy and reorienting behavior among the brushes showed significant differences as a result of degree of freedom of the flexible buffer chain spacers.

Keywords Azobenzene; block copolymers; diblock copolymer polymer brush; flexible spacer chain; grafted thin film; liquid crystalline polymer; optical anisotropy; photoorientation; surface-grafting; surface-initiated polymerization

1. Introduction

Surface modification using polymer brushes attract great interest for their effective tuning of surface properties such as wettability, switching, friction, and adhesion and so on [1–7]. In particular, surfaces with stimuli-responsive polymer brushes, also known as "smart surfaces" have attracted much attention in the last decade. The use of light as the external stimuli is particularly fascinating since remotely and accurately controls are feasible focusing onto specific areas. In this context, end-grafted polymer layers have been used as carriers for photo-responsive molecules, which exhibit surprisingly different properties from spin-casted films [8,9].

*Address correspondence to T. Seki, Department of Molecular Design and Engineering, Nagoya University, Furo-cho, Chikusa, Nagoya 464-8603, Japan. Tel.: +8152-789-4668, Fax: +82 52-789-4669. E-mail: tseki@apchem.nagoya-u.ac.jp

To fabricate more diversely responsive systems, diblock copolymer brushes have garnered enormous interest due to wide range of applications [10], which inter alia include modifications of adhesion [11], wettability [12], switching [13], stabilization [14], rheology [15], tribology [16] etc. For the preparation of diblock polymer brushes via grafting from the substrate surface, controlled radical polymerizations have offered many benefits, namely, control of the chain length (film thickness), uniformity of the brush surface, and the ability to produce brushes with complex architectures. The surface-initiated atom transfer radical polymerization (ATRP) technique [17] can be preferably used for this purpose.

Recently, we reported a diblock copolymer brush system consisting of a low glass transition temperature (T_g) coiled polymer block tethered to the substrate and a liquid crystalline chain block with an azobenzene (Az) mesogenic group as the outer layer. In the diblock copolymer brushes, the photoinduced motions of Az mesogens are significantly improved as a result of cooperative wiggling ascribed by the lubricant effect of the flexible chain spacer [18]. In the light of fascinating dynamic nature and effects of the buffer chain block as reported earlier, our next subject would be to elucidate the effect of flexible chain lengths. For better understanding, we will compare the structures and dynamic motional properties of the brushes of a P5Az10MA homopolymer and two BCP brushes having different lengths of PHMA flexible chains ($T_g = -20^\circ$C). Clear chain length effect of the flexible block is admitted in the dynamic photoorientation processes.

2. Experimental

Materials used for synthesis were of reagent grade and were purchased from TCI, Aldrich, and Kanto Kagaku. The azo chromophore containing a methacrylate monomer, 4-(10-methacryloydecyloxy)-4′-pentylazobenzene (5Az10MA), was synthesized according to the method previously reported [19]. A silane coupling reagent for the ATRP initiator, [11-(2-bromo-2-methyl)- propionyloxy] undecyldimethylchlorosilane (BUS), was synthesized according to method reported earlier [20]. The BUS modified substrate (quartz or silicon wafer) was prepared by the chemical vapor adsorption (CVA) method [21]. Typical ATRP conducting procedures are followed for fabricating di-block copolymer brushes step by step according to the previous report [18]. Scheme 1 illustrates the chemical structure of synthesized diblock polymer brush on a quartz substrate. As the chain length of the polymers can be controlled by monomer-initiator ratio, initial monomer concentration and the reaction time. We adopted the variation of monomer-initiator ratios to fabricate different lengths of PHMA chains. The feeding ratios for P5Az10MA were constant for all cases to get the same chain lengths of P5Az10MA layer, whereas for monomer-free initiator ratios between hexylmethacrylate (HMA) and free initiator, EBB (2-bromoisobutyric acid ethyl ester) were 500:1 and 1000:1 for brush-2 and brush-3 respectively.

2.1. Measurements

^{1}H NMR spectra were recorded on a JEOL 400GXS instrument spectrometer using tetramethylsilane as the internal standard for deuterated chloroform. Molecular weight and polydispersity index (PDI) of the free polymers were evaluated by gel permeation chromatography (GPC) using a Shodex liquid chromatography system. Layer thickness was measured by X-ray reflectivity (XRR) with a Rigaku ATX-G operating with Cu Kα radiation (0.154 nm). Grazing angle incidence X-ray diffraction (GI-XRD) measurements were performed with a Rigaku Nano Viewer operating with Cu Kα radiation (0.154 nm). UV-vis absorption

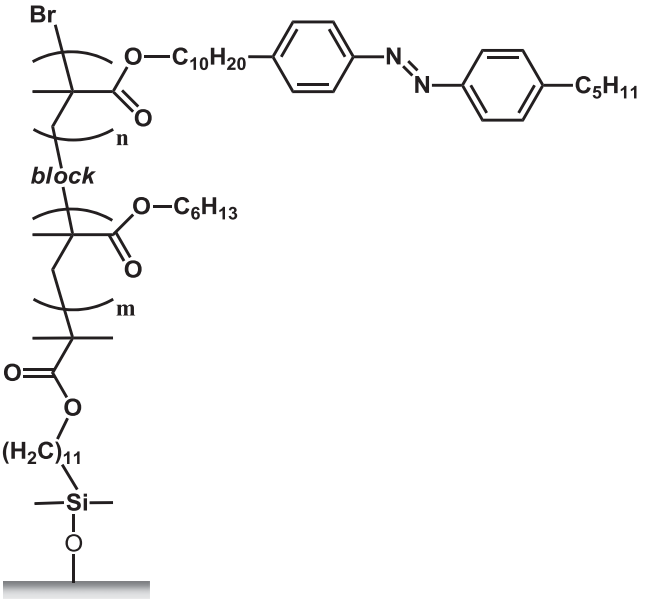

Scheme 1. Skeleton/chemical structure of synthesized PHMA-*b*-P5Az10MA diblock copolymer brush consisting of PHMA layer tethered to the quartz substrate (1st ATRP) and liquid crystalline Az-containing block (2nd ATRP) as surface layer.

spectra were recorded on an Agilent Technology 8453 spectrometer. To obtain polarized spectra, a polarizer was mounted in a rotating holder in front of the sample. The UV and visible light irradiation of the samples was performed using an Hg-Xe lamp (SAN-EI Electric UVF-203S) equipped with appropriate combinations of color filters (Toshiba glass: UV-35/UV-D36A and V-44/Y-43 for 365 and 436 nm light, respectively). Light intensity was measured by an optical power meter (Advantest TQ8210), and all LPL irradiation was performed at 1 mW cm^{-2}. Temperature of the sample plate was controlled with a Mettler FP82HT or a Heidolph MR Hei-Tec hot stage.

3. Results and Discussion

3.1. Synthesis of Surface-Grafted Diblock Copolymer Films

A smooth self-assembled monolayer (SAM) of a monofunctional organosilane compound of the initiator was successfully prepared by the CVA method. The chain length of PHMA block was varied by changing the monomer to free initiator feeding ratio. The characterizations of the polymers were analyzed by ^{1}H NMR and gel permeation chromatography. All M_w/M_n values ranged from 1.0 to 1.3, indicating that reasonably narrow dispersions of polymer masses were obtained by the ATRP method.

3.2. Structural Characterizations of Surface Brush Films

3.2.1. Film thickness. Film thicknesses were evaluated by the X-ray reflection (XRR) profiles, which provide well-coincided values with atomic force microscopic data [18]. Table 1 summarizes the film density, thickness and surface roughness for the P5Az10MA

Table 1. XRR profile of homo- and diblock copolymer brushes

Brush	Block	Density/ gcm^{-2}	Thickness/nm	Roughness/nm	Calculated length from DP/nm
brush-1	P5Az10MA	0.80	8	0.50	15
brush-2	PHMA (1st)	0.65	26	2.30	63
	P5Az10MA (2nd)	0.83	7	2.51	13
brush-3	PHMA (1st)	0.90	51	1.44	117
	P5Az10MA (2nd)	0.83	7.4	1.55	14

homopolymer brush (brush-1), and two PHMA-*b*-P5Az10MA diblock copolymer brushes (brush-2 and brush-3) obtained from the simulations of XRR data. As references, expected chain lengths assuming the ideally (all-zigzag conformation) stretched chain calculated from the degree of polymerization are also listed. As shown, the film thickness for these brushes was almost half of the fully stretched chains. These facts suggest that the brushes are not in a random coiled state but can be regarded as high density ones. P5Az10MA layer thicknesses were measured as 8.0 (homopolymer, brush-1), 7.0 (brush-2), and 7.4 nm (brush-3), which are comparable with each other. For PHMA layer thickness, brush-1, brush-2 and brush-3 were 0 nm, 26 nm and 51 nm, respectively. The brush-3 possessed almost doubled length of PHMA than the brush-2. So, the effect of thickness of the flexible buffer layer would be reasonably investigated by evaluating the three corresponding brushes, i. e., without a buffer layer (brush-1), and with the shorter (26 nm, brush-2) and the longer (51 nm, brush-3) flexible buffer chain.

3.2.2. Effect of flexible chain lengths on packing state and orientation of Az mesogens. Figure 1 shows UV-visible absorption spectra of brush-1 (a), brush-2 (b), and brush-3 (c) on quartz substrates taken with the perpendicular incidence for as-prepared state (solid lines) and after annealing at 130°C for 5 min (dashed lines). The LC Az homopolymer and diblock brushes showed the peaks around 240 and 340 nm, which are assignable to the $\varphi-\varphi^*$ transition of the aromatic ring and $\pi-\pi^*$ long-axis transitions of the Az unit, respectively. A slight hypsochromic peak shifts were observed for the $\pi-\pi^*$ absorption band in all three brushes than that in solution (352 nm), showing the partial formation of H-aggregates. After annealing, λ_{max} of the $\pi-\pi^*$ band of the brushes showed slight bathochromic shifts by 1 nm, 4 nm, and 6 nm, for brush-1, brush-2 and brush-3, respectively, to provide the almost the identical λ_{max} position (340–342 nm).

The spectral change after annealing was negligible for brush-1, but the $\pi-\pi^*$ absorption band exhibited significant increase for the block copolymer brushes (brush-2 and brush-3). The longer PHMA chain illustrated the larger spectral change. The relative intensity of absorption at the peak of $\pi-\pi^*$ band (ca. 340 nm) to that of $\varphi-\varphi^*$ one (ca. 240 nm) can be a measure of Az mesogen orientation [8,18] Change in the band ratio was listed in Table 2. The molecular orientation of LC Az units in the side chains had a nearly parallel orientation to the substrate for the high density P5Az10MA homopolymer and the diblock copolymer brushes as reported earlier [8,18]. We can interpret these findings in the following way. For P5Az10MA homopolymer brush, the Az mesogens were directly tethered from the substrate and thus degree of motional freedom is significantly poor. For this reason, Az mesogens cannot alter the aggregation state and their orientation is unaffected by the annealing. In the cases of diblock copolymer brushes, on the other hand, the flexible PHMA

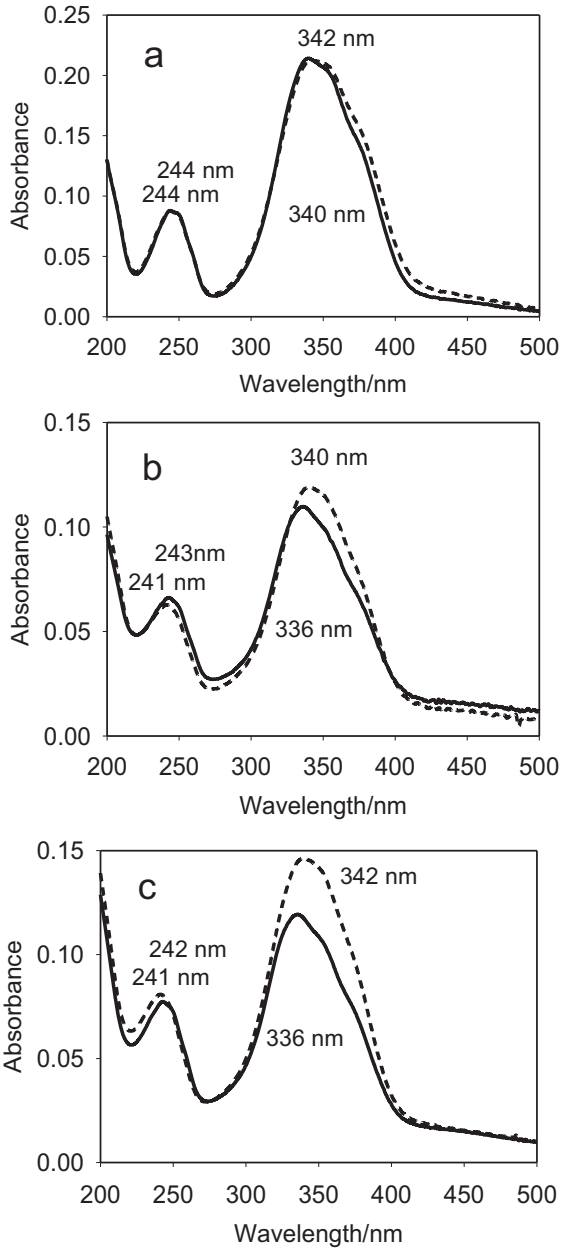

Figure 1. UV-vis absorption spectra of brush-1 (a), brush-2 (b) and brush-3 (c) on quartz substrates. λ_{max} values are shown in the figure. Solid and dashed lines indicate spectra before and after annealing at 130°C, respectively.

block chain provides freedom for out-of-plane reorientation. Here, the longer PHMA block chain (brush-3) leads to the larger reorientation. As for as-prepared diblock brushes, the orientation of Az is somewhat inclined in the upright direction, and the annealing leads to more laid orientation with the aid of the flexible PHMA chain almost to the same level of

Table 2. UV Spectral features of the brushes

Brush	Brush name	Annealing at 130°C	λ_{max} (π–π^*)	$A(\varphi-\varphi^*)/A(\pi-\pi^*)$
brush-1	P5Az10MA (8 nm) (n = 60)	Before	339	0.54
		After	340	0.57
brush-2	PHMA (26nm)-*b*-P5Az10MA (7 nm) (m = 258, n = 54)	Before	336	0.60
		After	340	0.52
brush-3	PHMA (51nm)-*b*-P5Az10MA (7.4nm) (m = 470, n = 58)	Before	336	0.77
		After	342	0.62

the homopolymer brush (brush-1). In short, the favorable packing and orientation states of Az mesogens are directly affected by the existence and length of flexible PHMA chains, and the higher the chain length leads to the higher the relaxation motions for the packing and orientation of the Az mesogenic groups. In contrast, the direct attachment of LC Az chains of P5Az10MA in the homopolymer system impedes such relaxations.

3.3. Photoinduced In-Plane Anisotropic Orientation with LPL

3.3.1. Photoinduced dichroism. Figure 2 shows polarized UV-vis absorption spectra of brush-1 (a), brush-2 (b), and brush-3 (c) after irradiation with 500 mJ cm^{-2} linearly polarized light (436 nm) at 70°C. The level of photoinduced in-plane optical anisotropy of films was evaluated by the order parameter (S) of the Az mesogens by S [$= (A_\perp - A_\parallel)/(A_\perp + 2A_\parallel)$], where $A_\perp$ and $A_\parallel$ denote absorbance at the λ_{max} (336 nm) obtained by the measurements using polarized light with E perpendicular ($\perp$) and parallel ($\parallel$) to that of actinic polarized light, respectively.

The highest S values in the optimized conditions for brush-1, brush-2 and brush-3 were 0.35, 0.48 and 0.53, respectively. The former study revealed that the degree of in-plane anisotropy depends on the thickness of the P5Az10MA layer [9,18]. As the P5Az10MA layers for all three brushes in the present study are comparable with respect to Az layer thickness, above differences in the photoinduced dichroism were accomplished only due to the higher degree of orientational freedom ascribed to the varied PHMA layers. The differences can also be correlated with the motional freedom possessed by the PHMA block chain. For the homopolymer brush (brush-1), the induction of molecular orientation is probably achieved on the free air side, and the Az mesogens in the vicinity of solid surface, probably in a range of a few nanometers from the surface. On the other hand, PHMA chains showed the ability to decouple the motional constraint from the solid surface and the extent of decoupling depends on the length of the PHMA chains. This obvious difference in the attainment of optical anisotropy ($S = 0.48$ and 0.53 for brush-2 and brush-3, respectively) can be ascribed due to extent of flexibility of PHMA chains connecting the P5Az10MA block.

3.3.2. Effect of temperature. The temperature dependence in attaining anisotropy was explored in more detail ranging from 20 to 110°C, and the results are displayed in Fig. 3. The largest S was obtained at around 80°C and 70°C for the homopolymer and diblock

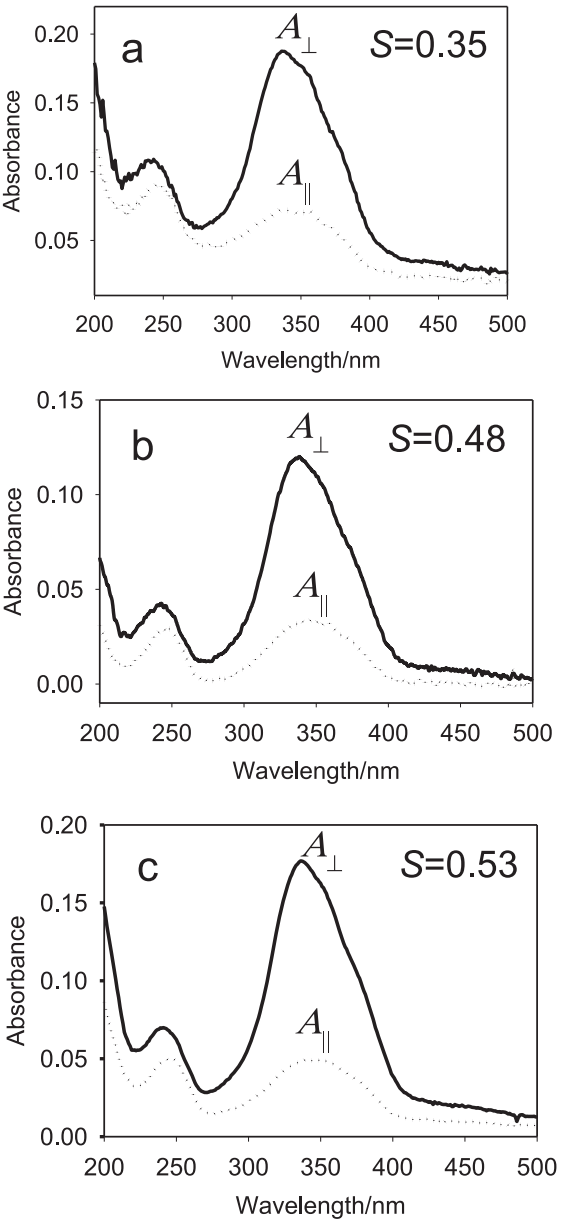

Figure 2. UV-vis absorption spectra of brush-1 (a), brush-2 (b) and brush-3 (c) after LPL irradiation with 500 mJ cm^{-2} at 70°C. Solid and dotted lines denote spectra taken with probing beams at a perpendicular and parallel incidence with the actinic LPL direction, respectively for all the cases.

copolymer brushes, respectively. These temperatures were slightly above the glass transition temperature of P5Az10MA chain to adopt the smectic A phase [8,18]. Thus, the high optical anisotropy requires the motional freedom for reorientation. With further temperature increase, *S* decreased again due to the orientational randomization Az mesogens with approaching to the isotropidization temperature around 100°C. As shown clearly, the

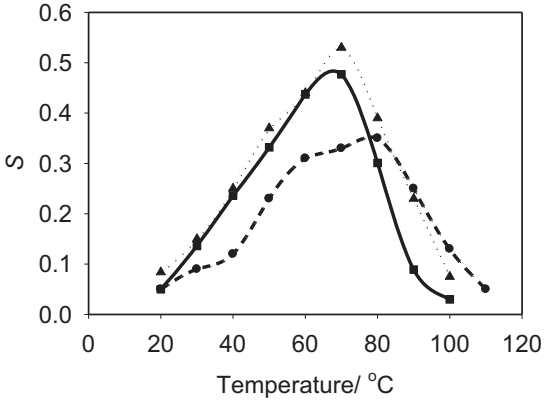

Figure 3. Orientational order parameters (S) obtained after 436 nm LPL irradiation at 500 mJ cm^{-2} varying the temperature for brush-1 (dash line), brush-2 (solid line), brush-3 (dot line).

diblock copolymer brushes gave the higher S values than that of the homopolymer at the optimum temperature range. Of the two diblock copolymer brushes, brush-3 possessing the longer PHMA block led to the larger S than brush-2.

The LPL-induced S in correlation with the PHMA is schematically summarized in Fig. 4. The existence of the buffer block of PHMA provides the higher orientational order of Az mesogens. Of the two block copolymer brushes, the longer PHMA improves the orientational order further possibly due to the more motional (conformational) freedom.

3.3.3. Structure evaluation by X-ray diffraction. GI-XRD measurements were performed for brush-2 in a similar way for brush-3 reported earlier [18]. The diblock brush was annealed at 130°C followed by a rapid cooling, and then the in-situ GI-XRD measurement was conducted at room temperature. The brush-2 exhibited diffraction peaks only in the in-plane direction at $2\theta = 2.52°$, which is attributed to a vertically oriented smectic layer

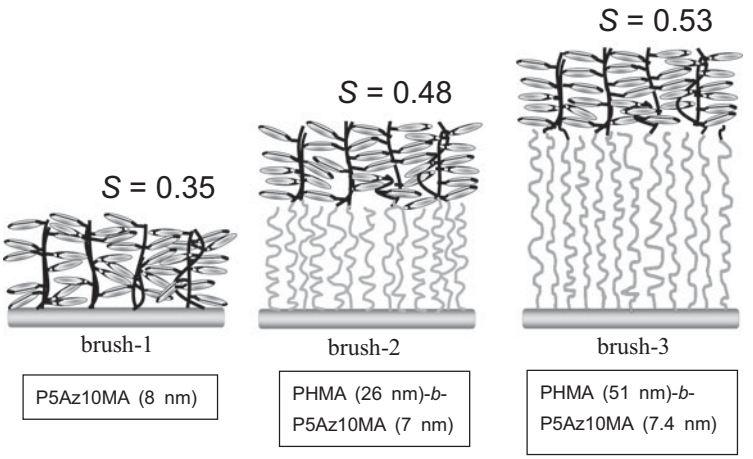

Figure 4. Comparative illustration of LPL induced optical anisotropy among brush-1, brush-2 and brush-3.

structure. The layer spacing ($d = 3.5$ nm) nearly coincided with the free polymer layer spacing and homopolymer grafted film of our previous report ($d = 3.6$ nm) [8,9]. No diffraction was observed with the incidence from orthogonal direction. The d spacings of the homopolymer brush [8] and the two diblock brushes were 3.6 nm [8,9], 3.5 nm and 3.4 nm [18], respectively. The differences are small but systematic. These results indicate that the more intrinsic assembling of Az mesogens are influenced by the length of flexible PHMA buffer chain and narrower interdigitated comb structure would be realized along with the PHMA length.

Temperature dependence of the GI-XRD data was obtained by in-situ measurements heating from 40°C to 100°C. In a similar way of our previous report for brush-3, the diffraction peak at $2\theta = 2.52°$ was observed for brush-2 until 90°C, but fully disappeared at 100°C. On the other hand, the peak disappeared for the homopolymer brush slightly above 110°C. This fact is consistent with the optical anisotropy data shown in Fig. 3. Not only the molecular orientation but also the layer structure is retained at the higher temperatures for the homopolymer brush due to the direct constraint from the solid substrate.

3.4. Photoinduced Reorientation

The in-plane rotational motions (reorientation) of Az mesogen to orthogonal polarization position were further examined and S at given irradiation conditions are shown in Fig. 5. S in the negative sign indicates the attainment of preferred orientation to the orthogonal direction.

At 20°C below T_g (a), no initial induction for reorientation was shown by brush-1 up to 500 mJcm^{-2}. In contrast, the both diblock brushes exhibited initial reduction of S within 200 mJ cm^{-2} due to the lubricant effect of the PHMA block. Prolonged irradiation at 3000 mJ cm^{-2} brought about considerable reduction in S in the three brushes. S was reduced to 0.20, 0.09 and 0.01, for brush-1, brush-2 and brush-3, respectively. Owing to the motional restriction from substrate surface, Az mesogens could not readily reorient in orthogonal direction for brush-1. On the other hand, 26 nm flexible chains in brush-2 induced some lubricant motions of Az mesogens and the more prominent reduction of anisotropy was observed. In case of brush-3, Az mesogens have almost fully lost their in-plane anisotropy in the macroscopic observation. This result is obviously an indication of the varied lubrication effect provided by the different lengths of PHMA flexible chains.

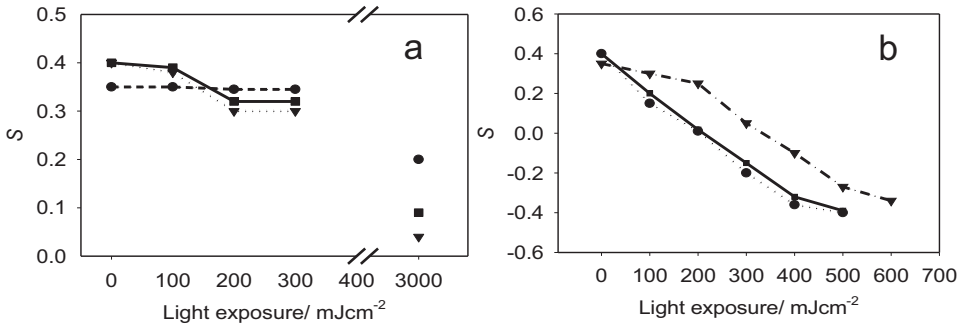

Figure 5. Change in the orientational order parameter (S) during the exposure to 436 nm LPL set orthogonal to the initial alignment at 20°C (a) and 70°C (b). Dashed, Solid and dotted lines are data forbrush-1, brush-2 and brush-3, respectively.

At 20°C, the successive LPL did not give the negative sign in *S*. Only the erasure of the initial orientation was performed.

On the contrary, at optimum temperature for the photoalignment (70°C), full reorientation behaviors were observed (b). There were no remarkable differences between the two diblock brushes in the reorientation behavior. Upon LPL irradiation, *S* immediately and linearly reduced until the full reorientation was achieved at 400 – 500 mJ cm^{-2}. For the homopolymer brush, on the other hand, non-linear behavior was observed. The reorientation was impeded at the initial stage until 200 mJ cm^{-2}, and then the reduction in *S* started, which should due to motional constraint from the surface at the initial stage. After this induction period, the reorientation process was readily occurred as a collective rotation of the Az mesogenic groups.

4. Conclusions

Surface-grafted block copolymer ultrathin films with different flexible layers have been successfully synthesized by two-step surface-initiated ATRP method where the surface block contains the photoreactive Az mesogenic units. The orientation of Az mesogenic groups were largely influenced by the existence and length of the buffer chain spacer, and the smectic layer structure was also become assembled more intrinsically with the cooperative wiggling ascribed to the flexible buffer layer. The role and effect of the length of flexible chains can be summarized as follows. (i) More efficient cooperative orientation of the Az liquid crystalline block is attained by the thicker PHMA layer in the diblock polymer brush. (ii) More intrinsic packing states have been achieved by the thicker buffer chain spacer. (iii) The rate of in-plane rotational motions, i. e., reorientation with orthogonal LPL irradiation at a lower temperature (20°C) is slightly enhanced by the thicker underlying flexible polymer chains in the diblock copolymer brush. In short, in addition to our previous work [18], this study further revealed the crucial roles of introduction of a flexible chain for the improvement of photoinduced motional functions of liquid crystalline Az mesogens in the surface tethered brush architecture by varying the length of the flexible buffer chain spacers and illustrated a significant difference of lubricant effect in the diblock copolymer brushes.

Acknowledgments

The authors thank Mr. T. Hikage, Dr. M. Hara, Mr. S. Kakehi and Mr. A. Nishimi for their support in conducting high intensity X-ray analysis. The research was supported by the Grant-In-Aid for Basic Research S (No. 23225003 to TS) from the Ministry of Education, Culture, Sports, Science and Technology, Japan, and PRESTO program (To SN) of Japan Science and Technology Agency.

References

[1] Zhao, B., Haasch, R. T., & MacLaren, S. (2004). *J. Am. Chem. Soc.*, *126*, 6124.
[2] Müller, M. (2002). *Phys. Rev. E*, *65*, 030802.
[3] Munirasu, S., Karunakaran, R. G., Rühe, J., & Dhamodharan, R. (2011). *Langmuir*, *27*, 13284.
[4] O'Driscoll, B. M. D., Griffiths, G. H., Matsen, M. W., & Hamley, I. W. (2011). *Macromolecules*, *44*, 8527.
[5] Minko, S. *et al.* (2003). *J. Am. Chem. Soc.*, *125*, 3896.
[6] Chen, T., Ferris, R., Zhang, J., Ducker, R., & Zausher, S. (2010). *J. Prog. Polym. Sci.*, *35*, 94.
[7] Tokarev, I., Motonov, M., & Minko, S. (2009). *J. Mater. Chem.*, *19*, 6932.

[8] Uekusa, T., Nagano, S., & Seki, T. (2007). *Langmuir*, *23*, 4642.
[9] Uekusa, T., Nagano, S., & Seki, T. (2009). *Macromolecules*, *42*, 312.
[10] Advincula, R. C., Brittain, W. J., Caster, K. C., & Rühe, J. (2004). (Ed.) *Polymer Brushes*, Wiley-VCH: New York.
[11] Lin, J. J. *et al*. (2004). *Langmuir*, *20*, 5493.
[12] Granville, A. M., & Brittain, W. (2004). *J. Macromol. Rapid Commun*., *25*, 1298.
[13] Camorani, P. *et al*. (2009). *Mol. Cryst. Liq. Cryst*., *502*, 56.
[14] Borukhov, I., & Leibler, L. (2002). *Macromolecules*, *35*, 5171.
[15] Semenov, A. N. (1995). *Langmuir*, *11*, 3560.
[16] Sakata, H., Kobayashi, M., Otsuka, H., & Takahara, A. (2005). *Polym. J*., *37*, 767.
[17] Matyjaszewski, K., & Xia, J. (2001). *Chem. Rev.*, *101*, 2921.
[18] Haque, H. A., Nagano, S., & Seki, T. (2012). *Macromolecules*, in press.
[19] Morikawa, Y., Kondo, T., Nagano, S., & Seki, T. (2007). *Chem. Mater.*, *19*, 1540.
[20] Ohno, K., Morinaga, T., Koh, K., Tsujii, Y., & Fukuda, T. (2005). *Macromolecules*, *38*, 2137.
[21] Hayashi, K., Saito, N., Sugimura, H., Takai, O., & Nagagiri, N. (2002). *Langmuir*, *18*, 7469.